Extended Abstracts of the 2016 International Conference on Solid State Devices and Materials, Tsukuba, 2016, pp515-516

M-2-03

Gate-controlled spin-orbit interaction in an InAs nanowire MOSFET

Keiko Takase[1], Yamato Ashikawa[1, 2], Guoqiang Zhang[1], Kouta Tateno[1], and Satoshi Sasaki[1, 2]

[1] NTT Basic Research Laboratory, NTT Corporation,
3-1, Morinosato-wakamiya, Atsugi, Kanagawa 243-0198, Japan
Phone: +46-240-3181 E-mail: takase.keiko@lab.ntt.co.jp
[2] Department of Physics, Tohoku University, Sendai 980-8578, Japan

Abstract

We report FET characteristics and magnetotransport of a gate-all-around InAs nanowire FET. The on/off ratio and the field-effect mobility are over 2500 and 600 cm^2/Vs at room temperature. Magnetoconductance measured at low temperature shows transition from weak localization to weak antilocalization caused by strong Rashba spin-orbit interaction modified by gate voltage. The estimated gate modulation of the Rashba coupling parameter is 1.5 × 10^{-11} eVm per volt. Such a large modulation rate would lead to an application to nanowire spin MOSFET.

1. Introduction

InAs is promising material to realize a practical spin FET because of high electron mobility due to small effective electron mass and large spin-orbit interaction. To control Rashba spin-orbit interaction proportional to electric field, nanowire FET has a preferable geometry, in which electrons are confined in a quasi-one-dimensional potential and thus gate can induce electric field more effectively. However conventional back-gated InAs nanowire FETs [1-4] employed SiO_2 of the underneath substrate as a gate insulator, and thus the voltage required to substantially modify the spin-orbit interaction length in the InAs channel often exceeds 10 V, giving a challenge to industrial application favoring low-power consumption.

Here we report on a MOS-type InAs nanowire FET using a gate-all-around (GAA) structure with thin high-κ gate dielectrics. This enables typical gate electric field applied to the channel to be ~ 1× 10^{7}V/m, which is larger than that for back-gated nanowire FETs by one order of magnitude for the same applied gate voltage. The spin-orbit interaction length (l_{so}) in our device is estimated from magnetotransport exhibiting transition from weak localization to weak antilocalization. It is found that l_{so} is changed by 100 nm in a sub-voltage via the gate, corresponding to the Rasha coupling parameter variation of ~1.0 × 10^{-11} eVm. Our results demonstrating gate-control of Rasha coupling parameter can open up a route to development of practical MOS nanowire spin FET.

2. Experimental

The sample is fabricated from InAs nanowire which was grown by VLS method. As shown in Fig. 1(a), the area covered by the gate electrode is more than 90 % of the channel length between source (S) and drain (D), allowing us to neglect contributions of the ungated regions and the contacts. To fabricate GAA structure [Fig. 1(b)] to induce strong electric field on the channel, Al_2O_3 (2 nm) and HfO_2 (4 nm) were first grown by ALD around the nanowire. The coated wire was then transferred to SiO_2/Si substrate with prepatterned metal gate, and was successively subject to additional deposition of metal gate. This two-stage deposition of metal enables formation of the gate-all-around structure shown in Fig. 1(b). The details of the fabrication method were reported in Refs. [5] and [6]. The electrical characterization of FET performance was conducted at room temperature, and magnetotransport measurement to investigate spin-orbit interaction was carried out at around 1.5 K.

3. Results and discussion

Figure 1(c) shows transfer characteristics of our GAA InAs nanowire FET taken at room temperature at source-drain voltage (V_{sd}) of 300 mV. When the gate voltage (V_g) increases from -2 V, the source-drain current (I_{sd}) rapidly increases around 0.6 V, showing transition from off to on state with on/off ratio of more than 2500. The peak mobility at V_g = 0.6 V is ~600 cm^2/Vs. These values are comparable to those of previously reported various types of InAs nanowire FETs [7,8]. Figure 1(d) shows I_{sd} as a function of V_{sd} at V_g = 0.8 and 1.2 V at room temperature and 1.5 K. Linear I_{sd} - V_{sd} features are shown up to V_{sd} ~ 0.1 V for both temperatures.

We next turn to magnetotransport measurements taken at ~1.5 K to investigate the effect of the spin-orbit interaction

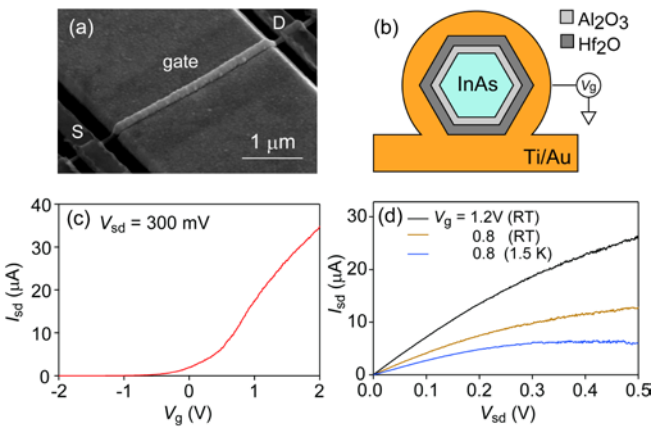

Fig. 1 (a) Scanning electron microscope image of our device. (b) Schematic illustration of a cross section of the device. (c) I_{sd} as a function of V_g measured at room temperature. (d) I_{sd} as a function of V_{sd} measured at room temperature and 1.5 K.

on the nanowire channel. Figure 2 shows correction of magnetoconductance (ΔG) as a function of the magnetic field (B), where the magnetoconductance was deduced from two-terminal dc-transport at V_{sd} = 10 mV. The data shown in Fig. 2 have been smoothed over V_g ±15 mV and B ±15 mT to exclude universal conductance fluctuations or other fluctuations due to impurities, as was done in Refs. [2] and [3]. In addition, our data are further averaged with respect to reversed magnetic field sweep direction to make the data fitting more reliable. At V_g = 0.24 V, ΔG increases upon application of B, whereas at V_g = 0.87 V, ΔG first decreases and turns to increase. This indicates a transition from weak localization to weak antilocalization, which was known to occur in the presence of strong spin-orbit interaction due to interplay between the spin-orbit interaction length and the phase coherence length (l_ϕ) [9].

Such a transition from weak localization to weak antilocalization was previously observed for various types of InAs nanowire devices: back-gated FETs measured individually [2] or in parallel [1], a suspended nanowire [8], double gated one [10] and ion-gated nanowire [10]. For these devices, mean fee path is smaller than nanowire diameter, and thus l_{so} and l_ϕ was deduced using the following equation describing correction of magnetoconductance in one-dimensional disordered metallic channel [7],

$$\Delta G = -\frac{2e^2}{hL_g}\left[\frac{3}{2}\left(\frac{1}{l_\phi^2}+\frac{4}{3l_{so}^2}+\frac{1}{D\tau_B}\right)^{-1/2}-\frac{1}{2}\left(\frac{1}{l_\phi^2}+\frac{1}{D\tau_B}\right)^{-1/2}\right] \quad (1)$$

where e is electron charge, h is Plank constant, L_g is gate length, D is diffusion constant, and τ_B is magnetic relaxation time. Here τ_B is given by

$$\tau_B = \frac{3l_B^{\,4}}{W^2 D} \quad (2)$$

with l_B being magnetic length given by $l_B = \sqrt{h/2\pi eB}$. Note that this reduces the fitted parameters to be only l_{so} and l_ϕ.

Regarding our device, the mean free path is ~ 12 nm and is smaller than the nanowire diameter of 100 nm. Therefore, Eq. (1) is used to nicely fit our data as shown in Fig. 2(a). Estimated l_{so} and l_ϕ are ~140 and 270 nm at V_g = 0.24 V, and ~190 and 130 nm at V_g = 0.87 V. Note that the relative magnitude of l_{so} and l_ϕ directly correlates to the transition

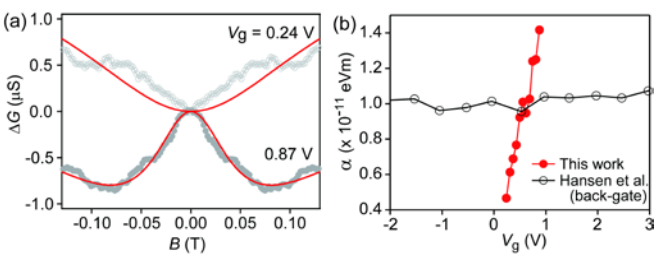

Fig. 2 (a) ΔG plotted as a function of B obtained for V_g = 0.24 V and 0.87 V. Solid lines indicate fitted curves. (b) Rashba coupling parameter α vs. V_g. For comparison, α of back-gated InAs nanowire FET was calculated from l_{so} in Ref. [1].

from weak localization to weak antilocalization, as pointed out in Ref. [3]. V_g dependence of Rashba coupling parameter α, defined as $\alpha = \hbar^2/(2m^* l_{so})$ with ħ being reduced Planck constant, is plotted in Fig. 2(b). As shown clearly, our device enables to change α much more efficiently than back-gated InAs nanowire FETs [1]. Such high tunability of the Rashba coupling parameter will contribute to open up a route to application of nanowire spin FETs.

3. Conclusions

We report electrical transport of a GAA InAs nanowire FET using high-κ gate insulator. It shows on/off ratio of more than 2500 and the field-effect mobility of 600 cm^2/Vs. Our FET also demonstrates high gate tunability of the spin-orbit interaction length and the Rashba coupling parameter.

Acknowledgements

We acknowledge H. Murofushi for technical support on fabrication of devices. .

References

[1] A. E. Hansen, M. T. Björk, C. Fasth, C. Thelander, and L. Samuelson, Phys. Rev. B **71**, 205328, (2005).

[2] S. Dhara, H. S. Solanki, V. Singh, A. Narayanan, P. Chaudhari, M. Gokhale, A. Bhattacharya, and M. M. Deshmukh, Phys. Rev. B **79**, 121311, (2009).

[3] P. Roulleau, T. Choi, S. Riedi, T. Heinzel, I. Shorubalko, T. Ihn, and K. Ensslin, Phys. Rev. B, 81, 155449 (2010).

[4] S. Estévez Hernández, M. Akabori, K. Sladek, C. Volk, S. Alagha, H. Hardtdegen, M. Pala, N. Demarina, D. Grützmacher, and T. Schäpers, Phys. Rev. B, **82** 235303 (2010).

[5] S. Sasaki, K. Tateno, G. Zhang, H. Suominen, Y. Harada, S. Saito, A. Fujiwara, T. Sogawa, and K. Muraki, Appl. Phys. Lett., 103, 213502 (2013).

[6] S. Sasaki, K. Tateno, G. Zhang, H. Pigot, Y. Harada, S. Saito, A. Fujiwara, T. Sogawa, and K. Muraki, Jpn. J. of Appl. Phys. 54, 04DN04 (2015).

[7] S. Dhara, S. Sengupta, H. S. Solanki, A. Maurya, A. Pavan R., M. R. Gokhale, A. Bhattacharya, and M. M. Deshmukh, "Facile fabrication of lateral nanowire wrap-gate devices with improved performance," Appl. Phys. Lett., vol. 99, no. 17, 2011.

[8] Q. Li, S. Huang, D. Pan, J. Wang, J. Zhao, and H. Q. Xu, Appl. Phys. Lett., 105, 113106 (2014).

[9] S. Hikami, A. I. Larkin, and Y. Nagaoka, Prog. Theor. Phys. **63**, 707 (1980).

[10] D. Liang and X. P. A. Gao, Nano Lett., **12**, 3263 (2012).